Steel and Composite Structures, *Vol. 36, No. 2 (2020) 213-228*
DOI: https://doi.org/10.12989/scs.2020.36.2.213

Analysis of extended end plate connection equipped with SMA bolts using component method

Ali Toghroli[1], Mohammad Sadegh Nasirianfar[2], Ali Shariati*[3,4], Majid Khorami[5], Masoud Paknahad[6], Masoud Ahmadi[7], Behnam Gharehaghaj[8] and Yousef Zandi[8]

[1]*Institute of Research and Development, Duy Tan University, Da Nang 550000, Vietnam*
[2]*Historic Building Rehabilitation (HBR), School of Architectural Engineering, University of Bologna, Ravenna 48121, Italy*
[3]*Division of Computational Mathematics and Engineering, Institute for Computational Science, Ton Duc Thang University, Ho Chi Minh City 758307, Vietnam*
[4]*Faculty of Civil Engineering, Ton Duc Thang University, Ho Chi Minh City 758307, Vietnam*
[5]*Universidad UTE, Facultad de Arquitectura y Urbanismo, Calle Rumipamba s/n y Bourgeois, Quito, Ecuador*
[6]*Faculty of Engineering, Mahallat Institute of Higher Education, Mahallat, Iran*
[7]*Department of Civil Engineering, Ayatollah Boroujerdi University, Boroujerd, Iran*
[8]*Department of Civil Engineering, Tabriz Branch, Islamic Azad University, Tabriz, Iran*

(*Received February 19, 2020, Revised May 17, 2020, Accepted May 26, 2020*)

Abstract. Shape Memory Alloys (SMAs) are new materials used in various fields of science and engineering, one of which is civil engineering. Owing to their distinguished capabilities such as super elasticity, energy dissipation, and tolerating cyclic deformations, these materials have been of interest to engineers. On the other hand, the connections of a steel structure are of paramount importance because of their vulnerabilities during an earthquake. Therefore, it is indispensable to find approaches to augment the efficiency and safety of the connection. This research investigates the behavior of steel connections with extended end plates equipped hybridly with 8 rows of high strength bolts as well as Nitinol superelastic SMA bolts. The connections are studied using component method in dual form. In this method, the components affecting the connections behavior, such as beam flange, beam web, column web, extended end plate, and bolts are considered as parallel and series springs according to the Euro-Code3. Then, the nonlinear force- displacement response of the connection is presented in the form of moment-rotation curve. The results obtained from this survey demonstrate that the connection has ductility, in addition to its high strength, due to high ductility of SMA bolts.

Keywords: extended end plate connection; shape memory alloy; moment-rotation curve; superelastic behavior; component method

1. Introduction

Since last decades, studying the behavior of connections in steel moment frames in seismic regions has been a subject of interest to civil engineers. However, serious and scrutinizing assessments were carried out after Northridge (California 1994) and Kobe (Japan 1995) earthquakes. In these events, steel buildings had been damaged mostly due to the failure occurred in the welding region of beam to column connections. These earthquakes motivated the researchers to re-evaluate the designing conventional philosophy. In this regard, Federal Emergency Management Agency (FEMA) (Venture 1997) embarked on a six year project known as SAC to investigate and improve the reliable and efficient methods for controlling, evaluating, repairing, and strengthening of steel moment frames. According to the results obtained from this research, weak performances of the connections are due to the assumptions of design, the properties of applied materials, and mostly the execution procedure. Consequently, the researchers recommended the application of the connections with end plates rather than conventional weld ones taking the philosophy of strong column-weak beam into account.

The merits of such connections are their appropriate strength, rigidity, and ductility; and their demerits can be referred to the residual deformations after earthquakes, high cost, and difficult repair and reconstruction. The researchers have proposed several solutions to remove the residual deformations after earthquakes. Researches by (Christopoulos *et al.* 2002, Ricles *et al.* 2002) used high strength post-tensioned steel bars to form the self-centering mechanism. Meanwhile, several suggestions such as shape memory alloys have been presented to change the properties of materials. Shape memory alloys have been specifically considered since the past two decades; the most used of which is Nitinol. These materials with the capability of tolerating high strains up to about 8% are utilized in dampers, braces, base isolators, and beam to column and column to foundation connections. Recently, several researchers have done research into the shape memory alloys (SMA). In addition (Ocel *et al.* 2004) used SMA bars in the semi-rigid beam to column connection. These connections have been controlled during two tests in which

*Corresponding author, Ph.D.
E-mail: alishariati@tdtu.edu.vn

http://www.techno-press.org/?journal=scs&subpage=8
ISSN: 1229-9367 (Print), 1598-6233 (Online)

four SMA bars are employed to transmit the loads of beam to the column with the connection of beam flange to column flange. In the first test, the energy dissipation capacity, high ductility, and strength changes have been evaluated in the initial cycles. According to the obtained results, the connections show high capacity of energy dissipation, high ductility, and slight strength change. Then, the SMA bars have been diverted to their primary statuses to investigate the recursive cyclic behavior of the connection. The obtained results have indicated the stability of connections.

Shear connectors are the most economical connectors in composite floor systems, especially because of the easy installation process, which do not require adept workers. Seismic performance of the connectors in the composite floor systems depends on concrete slab quality and shear connectors type, in order that a connector with high strength concrete slab shows the elastic-plastic behavior (Shariati *et al.* 2010, Shariati *et al.* 2011, Shariati *et al.* 2011, Shariati *et al.* 2011, Shariati *et al.* 2012, Shariati *et al.* 2012, Shariati *et al.* 2012, Shariati 2013, Shariati *et al.* 2014, Khorramian *et al.* 2015, Shariati *et al.* 2015, Khorramian *et al.* 2016, Shahabi *et al.* 2016, Shahabi *et al.* 2016, Shariati *et al.* 2016, Tahmasbi *et al.* 2016, Khorramian *et al.* 2017, Hosseinpour *et al.* 2018, Nasrollahi *et al.* 2018, Paknahad *et al.* 2018, Wei *et al.* 2018, Davoodnabi *et al.* 2019).

Different loading scenarios have been employed to simulate the seismic loading such as horizontal shaking by shake table test, vertical shaking and universal machine loading. Each of the loading plans is divided into two main categories, either monotonic or cyclic loading. In monotonic loading, the linear response of the structure is obtained while in cyclic loading, the hysteresis and nonlinear response would be achieved. Cyclic loading has been performed in two different styles; fully cyclic and half cycle. Generally, wherever the specimens cannot be subjected to fully cyclic loading, the half-cycle loading is employed. Different types of connections and structural components have been investigated and examined under monotonic or cyclic loadings so that the shear connectors (especially the C shaped connectors) have demonstrated an appropriate energy dissipation during cyclic loading and through hysteresis patterns (Shariati *et al.* 2012, Shariati *et al.* 2012, Shariati *et al.* 2013, Shariati *et al.* 2014, Shariati *et al.* 2017, Shariati *et al.* 2020).

Seismic performance of the buildings depends on the performance of its components under seismic loadings. Connections are the most central parts of each support, and during an earthquake, the strength of the fasteners, bolts or nuts should determine the proficiency of the connection (Arabnejad Khanouki *et al.* 2010, Jalali *et al.* 2012, Khorami *et al.* 2017, Khorami *et al.* 2017).

The dynamic behavior of the connection has been studied in the second test. With regard to the obtained results, the connection has shown the behavior similar to the quasi-static behavior, excluding its reduction of energy dissipation. The connections similar to the superelastic SMA bars have been studied by (Penar) showing appropriate recentering capacity. (Abolmaali *et al.* 2006) scrutinized the cyclic behavior of T-stub connections equipped with SMA bolts showing proper energy dissipation and recentering. (Ma *et al.* 2008, Ma *et al.* 2007) modeled and analyzed an extended end plate connection equipped with shape memory bolts using ANSYS software. They observed that the energy capacity and ductility were improved due to the superplastic property of SMA bolts as well as the formation of plastic hinge in the connection face. Moreover, other structural members such as beam, column, and end plate remained elastic after earthquake, preventing the cost and difficulties of repairing. (Hu *et al.* 2011) suggested a new method of steel beam to CFT column connection (the tubes filled with concrete) using SMA cables along the whole length of the column, accompanied with an analytical model for several types of connections. (DesRoches *et al.* 2010, Ellingwood *et al.* 2010) studied the moment frames equipped with SMA connections using finite element method and nonlinear time history analysis. They also assessed the effects of several connections on the permanent inter-storey drift, obtaining considerable results such as reduction of inelastic displacements. (Fang *et al.* 2014) continued the works of Ma et al. on the connections with extended end plates. They replaced high strength bolts by SMA bolts in the connections, performing 8 experimental tests, 7 with SMA bolts and 1 with high strength bolts.

They focused on the stiffness, strength, energy dissipation, and ductility of such moment connections in the length and diameter of different bolts. They figured out the formation of plastic hinge in the connection face because of the superelastic property of Naitinol bolts. (Wang and Chen 2009) presented a new connection between I-shape beam and CHS column equipped with SMA and steel bars. They studied the recentering and energy dissipation capacities of these connections numerically as well as experimentally. Their tests properly demonstrated the significance of the thickness of steel angles applied as stiffener. Accordingly, the connections with thicker angles or so called the connections with higher stiffness showed higher energy dissipation and recentering. They proved that the connections equipped with SMA bars of higher prestressing force presented more appropriate recentering. (Fanaie and Monfared 2016) studied the cyclic behavior of steel connections with extended end plate equipped with 8 bolt rows of shape memory alloy. In the mentioned research, the conventional connections with high strength bolts were compared to the ones equipped with SMA bolts. They concluded that the connections with Nitinol bolts had good recentering in addition to high energy dissipation capacities and ductility

2. The basis of shape memory alloys

Shape memory alloys (SMA) or intelligent alloys have been primarily presented by (Ölander 1932) and shape memory topic by (Vernon and Vernon 1941) for dental polymeric materials. The importance of shape memory material remained unknown until 1962 when (Buehler *et al.* 1963) found its effectiveness in the Nickel-Titanium alloy. This material was called Nitinol, referring to NiTi composition as well as its discovery location (Naval

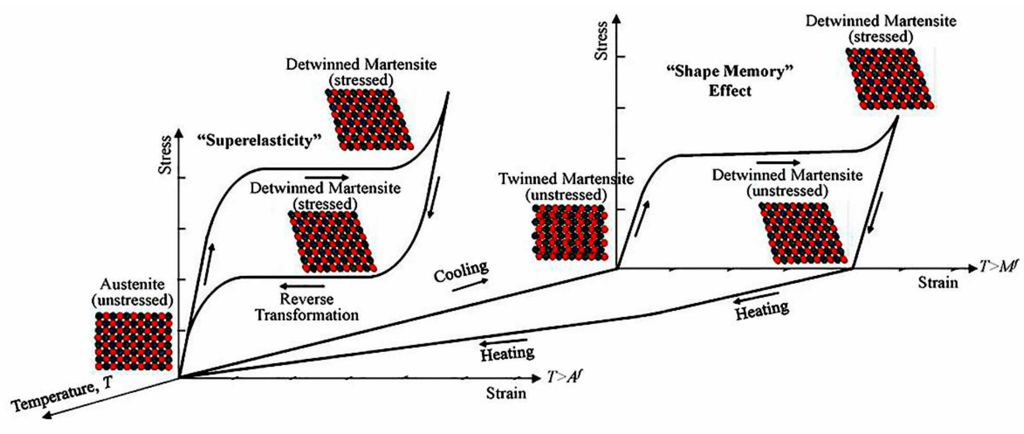

Fig. 1 The behavior of Nitinol shape memory alloy under different temperatures and stresses

Ordnance Laboratory). Since then shape memory alloys, the intelligent devices, have drawn the attention of researchers, particularly civil engineers, as passive structural control systems. One of the properties of these alloys which makes them unique is their recentering immediately after unloading (the effect of superelastic) or by heating (the effect of shape memory). These effects are due to the alterations of crystalline phase of these alloys. Shape memory alloys possess two stable phases,namely, martensite, in low temperature; and austenite, in high temperature. These two phases can be converted to each other through applying stress and temperature. So far, different types of shape memory alloys have been presented; the most important ones are copper- aluminum-nickel and nickel- titanium (Nitinol). They are very applicable in civil engineering. In this research, Nitinol is assessed considering its stability, high application, and thermomechanical application.

2.1 Superelastic effect (SE)

As illustrated in Fig. 1, if Nitinol is deformed in the temperature higher than that of austenite phase (A_f), the created deformations can be removed after unloading and the change of crystalline arrangement in the martensite phase can bring about energy dissipation. This phenomenon is known as superelastic effect (SE).

2.2 Shape memory effect (SME)

According to Fig. 1, if Nitinol is loaded and unloaded in the martensite phase, the material does not return to its initial status after unloading; and a residual deformation remains in it. The created residual deformation is removed by applying the temperature higher than A_f; and the material returns to its initial state. This phenomenon is known as shape memory effect (SME).

3. Introducing the component method

In the recent decades, the behavior of flexural connections with extended end plate has been evaluated through numerical and experimental researches. In 1983, Ghassemieh *et al*. (1983) studied the behavior of flexural connections with extended end plate equipped with 8 bolts. (Sumner and Murray 2002) suggested a method for designing the connections with extended end plates, with and without stiffeners. (Gorgun 2013) proposed an analytical method for predicting the behavior of steel flexural frame with flexible members. (Baei) studied the flexibility of the connections with end plate using finite element method under seismic loading. Overcoming the analytical complexities of nonlinear finite element method in obtaining moment-rotation curve of steel flexural connections and finding their real behavior, urges simultaneous evaluation of their strength, stiffness and ductility. In this regard, (Standard) has presented component method. In this method, the connection response or so called moment-rotation curve is obtained in two steps. First, the individual components of the connection (Fig. 2(a)) are considered as springs (Fig. 2(b)) and evaluated according to EuroCode3 to obtain the responses. Bahadori and Ghassemieh (2015) performed a modified component method and studied the flexibility of connections in multiple steel moment frames. Their results show a good agreement with experimental and numerical methods. Then, these components are assembled in the form of parallel and series linear springs to derive the moment-rotation curve. In the current paper, the mentioned method is implemented for the connection with extended end plate and 8 bolt rows, Fig. 2.

Now, each spring or connection component has its own force-displacement parameter. The components of the connection are of three types, regarding their ductility: 1) with high ductility; 2) with brittle fracture; and 3) with limited ductility, presented in Figs 3 to 5.

Considering Fig. 2 and 3 to 5, the first types are: 1) column web in shearing; 2) column flange in bending; 3) end plate in bending; 4) beam web in tension. The second types are bolts in tension and shearing. The third types include: 1) column web in compression; 2) column web in tension; 3) web and flange of beam in tension. The strength and initial stiffness of the connection are calculated using the formulas

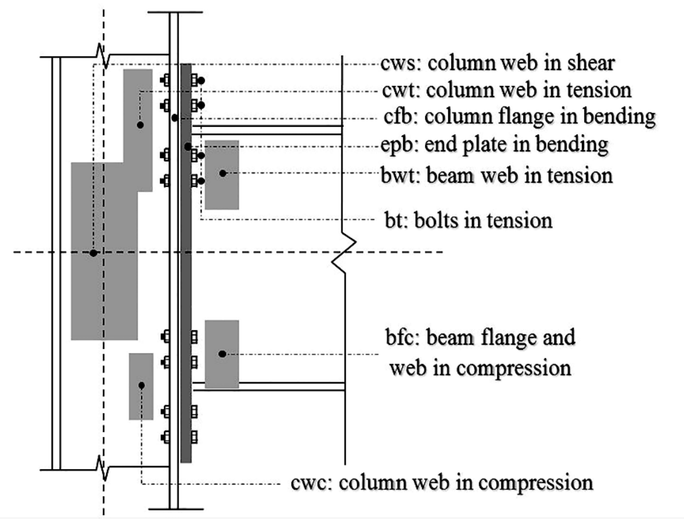

(a)

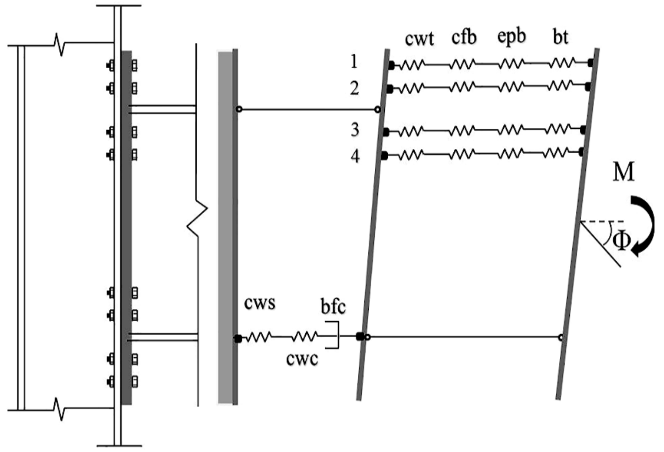

(b)

Fig. 2 Component of extended end-plate connection behavior; (a): Extended end plate connection and (b): Mechanical model for extended end plate connection (Aksoylar *et al.* 2011)

presented in Table 1, derived from Euro Code 3.

After calculating the strength and initial stiffness, presented in Table 1, the design flexural strength of connection ($M_{j,Rd}$) is obtained as follows

$$M_{j,Rd} = \sum h_r F_{tr,Rd} \tag{1}$$

Where, h_r is the distance of the r^{th} bolts from the center of compressive flanges of the beam $F_{tr,Rd}$ is the effective strength force of the r^{th} row, equal for each row with respect to the force of the series springs. Its value is considered equal to the lowest strength force of the components of the row. The rotational stiffness of the connection is calculated as follows

$$S_j = \frac{z_{eq}^2}{\mu K_{eq}} \tag{2}$$

Where, K_{eq} is the equivalent stiffness of the connection, obtained by Eq. (7); z_{eq} is the lever arm of the connection, calculated by Eq. (8); μ is the ratio of initial rotational stiffness to the rotational stiffness of the connection ($S_{j,ini}/S_j$), computed according to the section 6.3.1(6) and Table 6.8 of EuroCode3-part1.8, as follows

$$\mu = \begin{cases} \text{if } M_{j,Ed} \le \frac{2}{3} M_{j,Rd} \Rightarrow \mu = 1 \\ \text{if } \frac{2}{3} M_{j,Rd} < M_{j,Ed} \le M_{j,Rd} \Rightarrow \mu = \left(\frac{1.5 M_{j,Ed}}{M_{j,Rd}} \right)^{\psi} \end{cases} \tag{3}$$

Where, $M_{j,Ed}$ is bending moment applied to the connection; ψ= 2.7, from Table 6.8 presented in EuroCode3-part 1.8. Based on the Eqn 3, two different values are obtained for μ, proportional to which there will be initial and secondary rotational stiffness. To prevent the approximation, the curve should be plotted in trilinear form. Then, the stiffness of the connection is obtained as follows

$$\frac{1}{k_c} = \frac{1}{k_1} + \frac{1}{k_2} \tag{4}$$

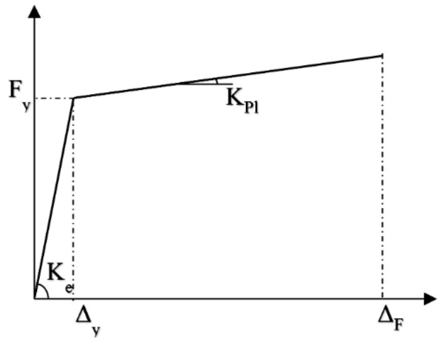

(a) Bilinear approximation model

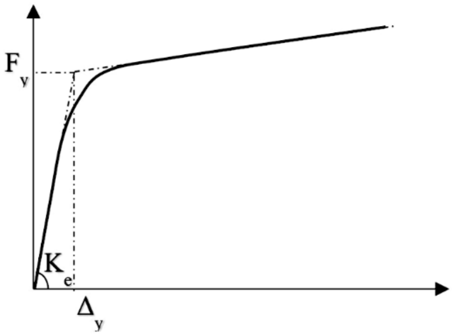

(b) Real model

Fig. 3 High ductility components (Da Silva and Coelho 2001)

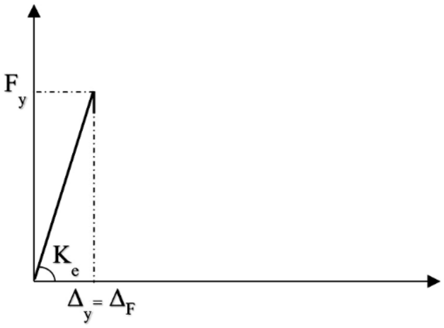

(a) Bilinear approximation model

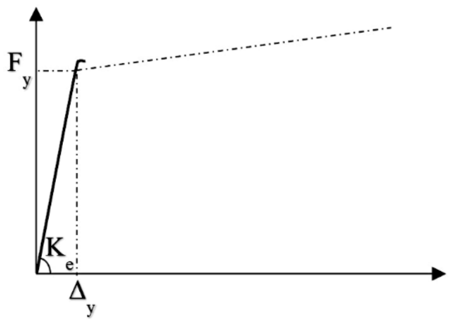

(b) Real model

Fig. 4 Brittle failure components (Da Silva and Coelho 2001)

$$\frac{1}{k_{t,r}}=\frac{1}{k_{3,r}}+\frac{1}{k_{4,r}}+\frac{1}{k_{5,r}}+\frac{1}{k_{10,r}} \tag{5}$$

$$k_t=\sum_{r=1}^{4}k_{t,r} \tag{6}$$

$$\frac{1}{K_{eq}}=\frac{1}{k_c}+\frac{1}{k_t} \tag{7}$$

$$z_{eq}=\frac{\sum_r k_{t,r}h_r^2}{\sum_r k_{t,r}h_r} \tag{8}$$

Where, k_1 and k_2 are the stiffness of column web in shear and compression, respectively, giving the equivalent stiffness of compressive part of the beam; $K_{3,r}$, $K_{4,r}$, $K_{5,r}$ and $K_{10,r}$ are the stiffness of column flange in bending, column web in tension, end plate in bending and bolts in tension, respectively, for the r^{th} row. They firstly give the equivalent stiffness of each row in tension ($K_{t,r,}$) and then its equivalent stiffness of tension part ($K_{t,}$). The symbols used in this study are summarized in Appendix A.

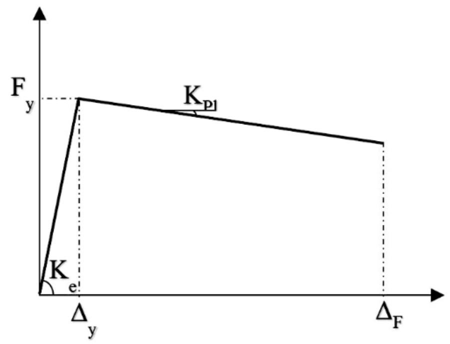

(a) Bilinear approximation model

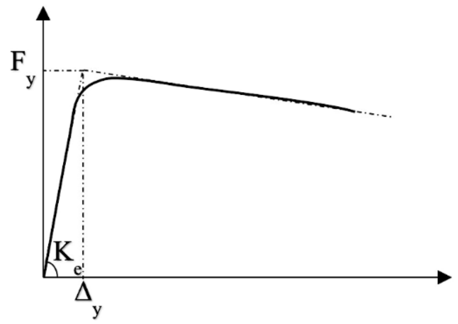

(b) Real behavior

Fig. 5 Limited ductility components (Da Silva and Coelho 2001)

The following assumptions are considered to obtain the behavior of the connection:

1- The end plate is exactly connected to the beam;
2- The behaviors of beam material, end plate and column are considered elastoplastic, as presented in Fig. 3;
3- The inter-plate displacement is ignored.
4- Ultimate bending moment is assumed equal to the yield bending moment.

4. Introducing and analyzing the model

4.1 The dimensions and materials

In this research the theoretical model of Fanaie and Nazari Monfared (2016) (Fig. 6) has been used to evaluate the suggested method. It should be mentioned that the outer 4 bolt rows are of SMA bolts with 7mm in diameter and the 4 inner ones are of high strength bolts with 21mm in diameter.

The materials used in the beam, column and end plate are of ST37 and those of high strength bolts are of ASTM325. Table 2 presents the mechanical properties of the connection components.

4.2 Calculating the needed parameters

The resisting force and initial stiffness of the connection components have been calculated according to Table 1 and presented in Table 3. It should be mentioned that 0.6fyAb pre-stressing force has been applied to the SMA bolts.

The parameters needed in Table 3 are calculated with respect to EuroCode3-part1.8 as follows:

Column web in shearing (CWS)

$A_{vc}=4800mm^2$

Column web in compression (CWC)

$b_{eff,c,wc}=194.48mm$

$\lambda_p=0.732\Rightarrow\rho=.993$

Web and flange of beam in compression (BFC)

$W_{pl}=1152000mm^2$

$M_{c,Rd}=251345.45kN.mm$

Column web in tension (CWT)

Other end bolt-row

$$\left.\begin{matrix}l_{eff,nc}=275.05mm\\ l_{eff,cp}=373.22mm\end{matrix}\right\}\xrightarrow{l_{eff,nc}<l_{eff,cp}}l_{eff,1}=l_{eff,2}=275.05mm$$

$b_{eff,t,wc}=l_{eff,1}=275.05mm$

Bolt-row adjacent to a stiffener

$$\left.\begin{matrix}l_{eff,nc}=433.62mm\\ l_{eff,cp}=373.22mm\end{matrix}\right\}\xrightarrow{l_{eff,nc}>l_{eff,cp}}l_{eff,1}=373.22mm$$

$b_{eff,t,wc}=l_{eff,1}=373.22mm$

Table 1 The formulas employed for calculating the strength and initial stiffness of the components

	Components	Strength	Initial stiffness
High Ductility	Column web in shear	$V_{wp,Rd} = \frac{0.9 \cdot f_{y,wc} \cdot A_{vc}}{\sqrt{3} \cdot \gamma_{M0}}$	$K_1 = \frac{0.38 \cdot A_{vc}}{\beta z} \cdot E$
	Column flange in bending	Equivalent T-stub model	$K_3 = \frac{0.7 \cdot b_{eff,t,wc} \cdot t_{wc}}{d_c} \cdot E$
	End plate in bending	Equivalent T-stub model	$K_5 = \frac{0.85 \cdot l_{eff} \cdot t_p^3}{m^3} \cdot E$
	Beam web in tension	$F_{t,wb,Rd} = \frac{b_{eff,t,wb} \cdot t_{wb} \cdot f_{y,wb}}{\gamma_{M0}}$	$K_8 = \infty$
Brittle Ductility	Bolts in tension	$F_{t,Rd} = \frac{0.9 \cdot f_{ub} \cdot A_s}{\gamma_{Mb}}$	$K_{10} = \frac{1.6 \cdot A_s}{L_b} \cdot E$
	Bolts in shear	According to bolts grade	$K_{11} = \frac{16 \cdot n_b \cdot d^2 \cdot f_{ub}}{E \cdot d_{M16}} \cdot E$
limited Ductility	Column web in compression	$F_{c,wc,Rd} = \frac{\omega \cdot b_{eff,c,wc} \cdot t_{wc} \cdot f_{y,wc}}{\gamma_{M0}}$ But $F_{c,wc,Rd} \le \frac{\omega \cdot \rho b_{eff,c,wc} \cdot t_{wc} \cdot f_{y,wc}}{\gamma_{M1}}$	$K_2 = \frac{0.7 \cdot b_{eff,c,wc} \cdot t_{wc}}{d_c} \cdot E$
	Column web in tension	$F_{t,wc,Rd} = \frac{\omega \cdot b_{eff,t,wc} \cdot t_{wc} \cdot f_{y,wc}}{\gamma_{M0}}$	$K_4 = \frac{0.85 \cdot l_{eff} \cdot t_{fc}^3}{m^3} \cdot E$
	Beam flange/ web in tension	$F_{c,wb,Rd} = \frac{M_{c,Rd}}{z}$	$K_7 = \infty$

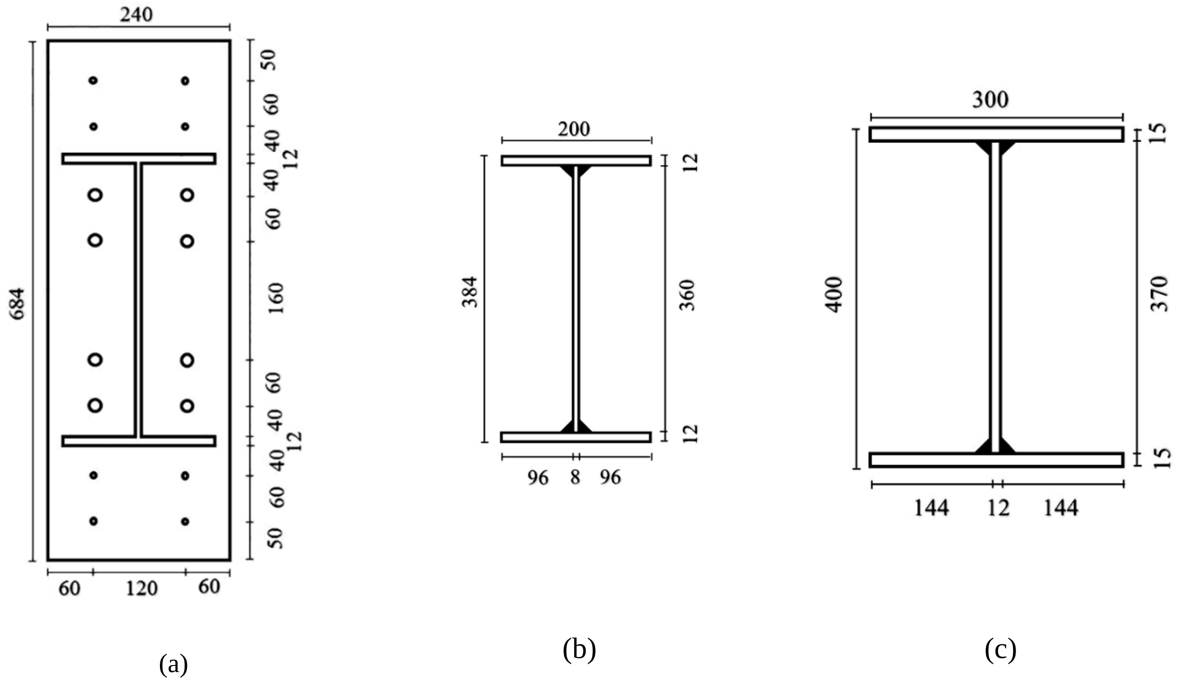

Fig. 6 Components of extended end-plate connection; (a): Extended end plate connection, (b): Beam Section and (c) Column Section

Table 2 Mechanical properties of connection elements

Material	**Elasticity Modulus (GPa)**	**Yielding stress (GPa)**	**Ultimate stress (GPa)**	**Poisson's ratio**
ST37	200	240	370	0.3
High strength bolt (ASTM325)	200	640	800	0.3
SMA bolts	42	370	500	0.33

Table 3 Strength and Stiffness coefficient of elements

			k(kN/mm)		**F(kN)**
Column web in shear	CWS	k_1	855	$V_{wp,Rd}$	544.18
Column web in compression	CWC	k_2	987.6	$F_{c,wc,Rd}$	442.42
Beam flange and web in compression	BFC	k	-	$F_{c,fb,Rd}$	698.18
Column web in tension	CWT	k_3	1212.97	$F_{t,cw,Rd}$	630.11
			1645.9		855
			1645.9		855
			1543.94		802.05
Column flange in bending	CFB	k_4	837.12	$F_{T,2,Rd}$	120.48
			1319.73		153.1
			1319.73		289.64
			1065.54		272.47
End plate in bending	EPB	k_5	865.71	$F_{T,2,Rd}$	107.79
			865.71		107.79
			2656.87		541.1
			2255.18		314.75
Bolts in tension	BT	k_{10}	517.24	$F_{s,Rd,ser}$	61.42
			517.24		61.42
			4655.1		399
			4655.1		399
Beam web in tension	BWT	k	-	$F_{t,wb,Rd}$	209.45
			-		209.45
			-		642.82
			-		545.63

Other inner bolt-row

$$\left.\begin{array}{l} l_{eff,nc}=350.1mm \\ l_{eff,cp}=373.22mm \end{array}\right\} \xrightarrow{l_{eff,nc}<l_{eff,cp}} l_{eff,1}=l_{eff,2}=350.1mm$$

$$b_{eff,t,wc}=l_{eff,1}=350.1mm$$

The column flange in bending (CFB)

Other end bolt-row

$$l_{eff,1}=l_{eff,2}=275.05mm \Rightarrow M_{pl,1,Rd}=M_{pl,2,Rd}=3375.61kN.mm$$

$$F_{T,1,Rd}=227.31kN$$

$$F_{T,2,Rd}=120.48kN$$

Bolt-row adjacent to a stiffener

$$\left.\begin{array}{l} l_{eff,1}=373.22mm \\ l_{eff,2}=433.62mm \end{array}\right\} \rightarrow \left\{\begin{array}{l} M_{pl,1,Rd}=4580.43kN.mm \\ l_{pl,2,Rd}=5321.7kN.mm \end{array}\right.$$

$$F_{T,1,Rd}=308.45kN$$

$$F_{T,2,Rd}=153.1kN$$

Other inner bolt-row

$$F_{T,1,Rd}=289.34kN$$

$$F_{T,2,Rd}=272.47kN$$

The end plate in bending (CFB)

Bolt-row outside tension flange of beam:

For rows 1 and 8

$$\left.\begin{matrix} l_{eff,nc} = 120mm \\ l_{eff,cp} = 434.16mm \end{matrix}\right\} \xrightarrow{l_{eff,nc} < l_{eff,cp}} l_{eff,1} = l_{eff,2} = 120mm$$

$$\Rightarrow M_{pl,1,Rd} = M_{pl,2,Rd} = 2618.19kN.mm$$

$$F_{T,1,Rd} = 176.31kN$$

$$F_{T,2,Rd} = 107.79kN$$

For rows 2 and 7

$$\left.\begin{matrix} l_{eff,nc} = 120mm \\ l_{eff,cp} = 155.66mm \end{matrix}\right\} \xrightarrow{l_{eff,nc} < l_{eff,cp}} l_{eff,1} = l_{eff,2} = 120mm$$

$$\Rightarrow M_{pl,1,Rd} = M_{pl,2,Rd} = 2618.19kN.mm$$

$$F_{T,1,Rd} = 176.31kN$$

$$F_{T,2,Rd} = 107.79kN$$

First bolt-row below tension flange of beam

For rows 3 and 6:

$$\left.\begin{matrix} l_{eff,nc} = 368.28mm \\ l_{eff,cp} = 373.22mm \end{matrix}\right\} \xrightarrow{l_{eff,nc} > l_{eff,cp}} l_{eff,1} = l_{eff,2} = 368.28mm$$

$$\Rightarrow M_{pl,1,Rd} = M_{pl,2,Rd} = 8035.2kN.mm$$

$$F_{T,1,Rd} = 541.1kN$$

$$F_{T,2,Rd} = 335.1kN$$

Other inner bolt-row

$$\left.\begin{matrix} l_{eff,nc} = 312.6mm \\ l_{eff,cp} = 373.22mm \end{matrix}\right\} \xrightarrow{l_{eff,nc} < l_{eff,cp}} l_{eff,1} = l_{eff,2} = 312.6mm$$

$$\Rightarrow M_{pl,1,Rd} = M_{pl,2,Rd} = 6820.36kN.mm$$

$$F_{T,1,Rd} = 459.28kN$$

$$F_{T,2,Rd} = 314.75kN$$

The bolts in tension (BT)

For rows 1, 2, 7 and 8

$$2A_s = 76.97mm^2$$

For rows 3, 4, 5 and 6

$$2A_s = 692.72mm^2$$

Beam web in tension (BWT)

In this component, the effective length is equal to the effective length calculated in the end plate component in bending

For rows 1 and 8

$$b_{eff,t,wb} = l_{eff,1} = l_{eff,2} = 120mm$$

For rows 2 and 7

$$b_{eff,t,wb} = l_{eff,1} = l_{eff,2} = 120mm$$

For rows 3 and 6

$$b_{eff,t,wb} = l_{eff,1} = l_{eff,2} = 368.28mm$$

For rows 4 and 5

$$b_{eff,t,wb} = l_{eff,1} = l_{eff,2} = 312.6mm$$

The stiffness values presented in Table 3 as well as the Eqs. (4) to (7), are used to calculate the equivalent stiffness of the connection expressed as follows:

$$\frac{1}{k_c} = \frac{1}{855} + \frac{1}{987.6} \Rightarrow k_c = 458.26\frac{kN}{mm}$$

$$\frac{1}{k_{t,1}} = \frac{1}{1212.97} + \frac{1}{837.12} + \frac{1}{865.71} + \frac{1}{517.24} \Rightarrow k_{t,1} = 195.79\frac{kN}{mm}$$

$$\frac{1}{k_{t,2}} = \frac{1}{1645.9} + \frac{1}{1319.73} + \frac{1}{865.71} + \frac{1}{517.24} \Rightarrow k_{t,2} = 224.53\frac{kN}{mm}$$

$$\frac{1}{k_{t,3}} = \frac{1}{1212.97} + \frac{1}{837.12} + \frac{1}{2656.87} + \frac{1}{4655.1} \Rightarrow k_{t,3} = 511.12\frac{kN}{mm}$$

$$\frac{1}{k_{t,4}} = \frac{1}{1543.94} + \frac{1}{1065.54} + \frac{1}{2255.18} + \frac{1}{4655.1} \Rightarrow k_{t,4} = 445.55\frac{kN}{mm}$$

$$k_t = \sum_{r=1}^{4} k_{t,r} = 195.79 + 224.53 + 511.12 + 445.55 = 1376.99\frac{kN}{mm}$$

$$\frac{1}{K_{eq}} = \frac{1}{k_c} + \frac{1}{k_t} = \frac{1}{458.26} + \frac{1}{1376.99} \Rightarrow K_{eq} = 343.84\frac{kN}{mm}$$

Considering the stiffness derived for each row and with respect to Eq. (8), the lever arm of the connection (z_{eq}) is defined as follows:

$$z_{eq} = 359.33mm$$

The initial rotational strength of the connection is expressed as follows:

$$S_{j,ini} = z^2 \times K_{eq} = \left(\frac{359.33}{1000}\right)^2 \times (343.84 \times 1000) = 44394.22kN.m$$

Design moment resistances as well as the rotation of yielding point are calculated as follows:

$$M_{j,Rd} = \sum h_r F_{tr,Rd}$$
$$= 61.42 \times 478 + 61.42 \times 418 + 289.64 \times 326 + 272.47 \times 266 = 221.93kN.m$$

$$\phi_y = \frac{M_{j,Rd}}{S_j} = 3.22E(-3)\,rad = 3.22mrad$$

The ultimate rotational capacity is obtained with respect to the article 6.4.2(2) of EuroCode3- part1.8, assuming enough rotational capacity in the connection, and also in accordance with the research conducted by Fanaie and Nazari Monfared (2016) as:

$$\varphi_u = 39.7mrad$$

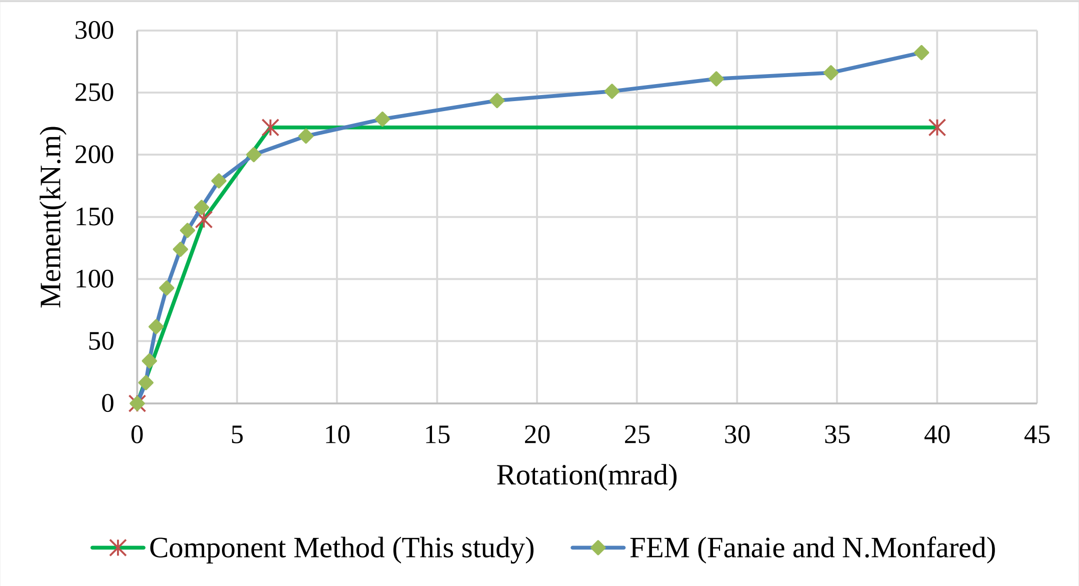

Fig. 7 Moment-Rotation Curve

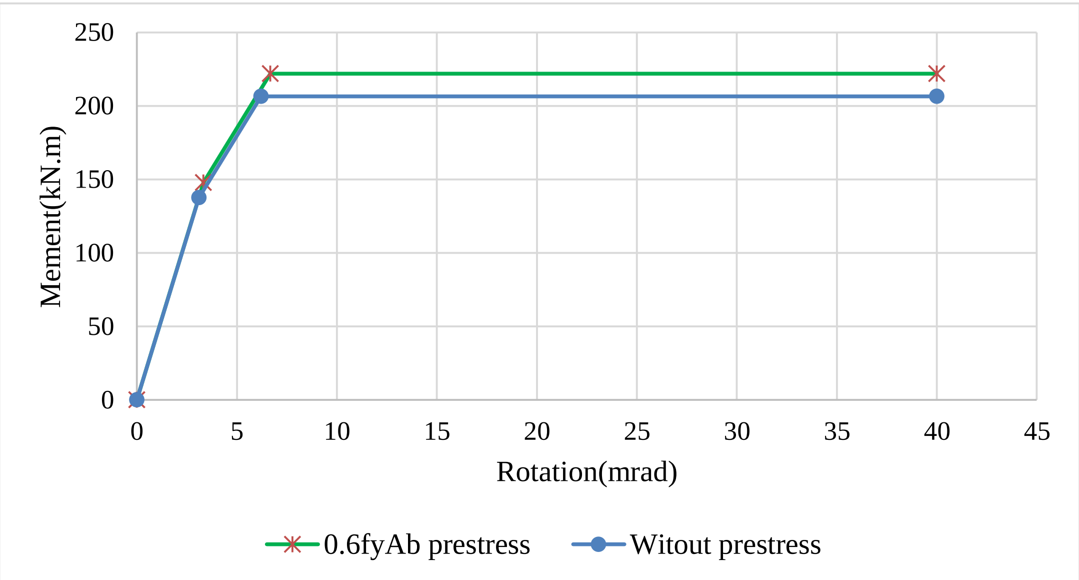

Fig. 8 The effect of pre stress on moment-rotation curve

5. Discussion

Four points are needed so as to plot trilinear moment-rotation curve: the initial point (0, 0), the point of yield moment ($\frac{\frac{2}{3}\cdot M_{j,Rd}}{S_{j.ini}}, \frac{2}{3}\cdot M_{j,Rd}$), yielding point ($\frac{\frac{2}{3}\cdot M_{j,Rd}}{S_{j.ini}} + \frac{\frac{1}{3}\cdot M_{j,Rd}}{S_j}, M_{j,Rd}$), and final point ($\varphi_u, M_u$) derived in the previous section. The moment-rotation curve has been plotted in Fig. 7.

In what follows several effective parameters of both curves are compared to study the accuracy of the method.

1) Initial rotational stiffness

$$\frac{44394.22 - 43773.93}{44394.22} \times 100 = 1.4\%$$

As it is observed the difference between calculated initial rotational stiffness is 1.4% based on the component method compared to the finite element method, which is very negligible.

2) The moment of yielding point

$$\frac{221.93 - 200.1}{221.93} \times 100 = 9.84\%$$

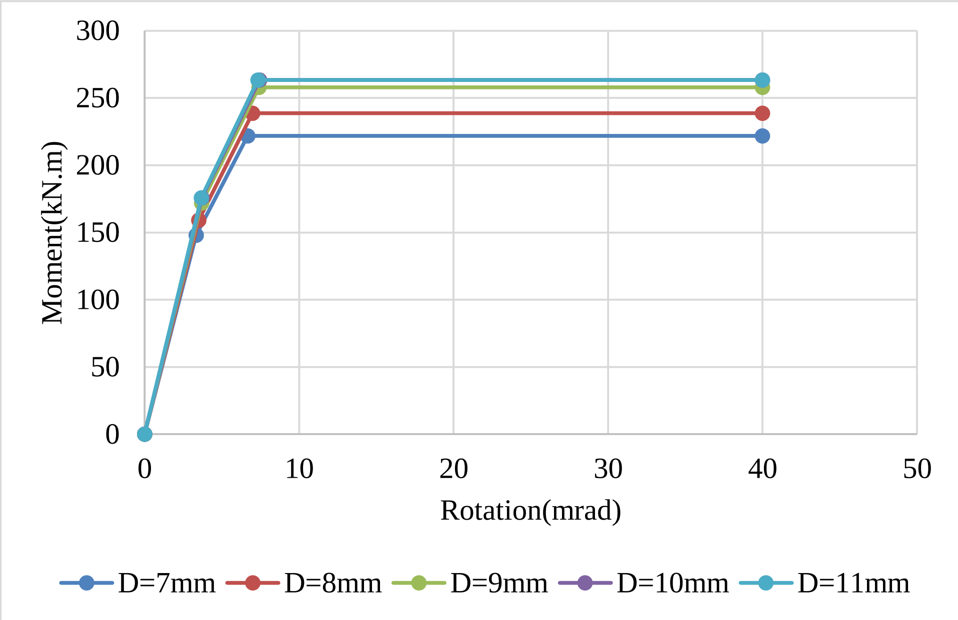

Fig. 9 The effects of bolt diameter on moment-rotation curve

Table 4 The effects of SMA bolts diameter on moment-rotation curve

Diametere (mm)	$M_{j,Rd}$ $(kN-m)$	$\frac{M_{j,Rd}-M_{j,Rd}(D=7mm)}{M_{j,Rd}}$	ϕ $(mrad)$	$\frac{\phi-\phi(D=7mm)}{\phi}$
7	221.93	-	6.67	-
8	238.78	7.06%	6.98	4.51%
9	257.87	13.94%	7.39	9.75%
10	263.48	15.77%	7.43	10.26%
11	263.48	15.77%	7.34	9.15%

The difference between calculated moments of yielding point is 9.84% based on the component method compared to the finite element method that is negligible.

3) The rotation of yielding point

$$\frac{6.66-5.83}{6.66}\times 100=12.46\%$$

The difference between calculated rotations in the yielding point of moment-rotation curve is 12.46% based on component method compared to the finite element method.

According to the performed comparison, the component method relatively shows good accuracy.

In what follows several parameters effective in the moment-rotation curve such as pre-stressing force and bolt diameter are investigated.

5.1 The effects of pre-stressing force

In order to assess this effect, Fig. 8 presents the moment-rotation curve for the status without pre-stressing force along with the previous status (with pre-stressing force of $0.6f_yA_b$).

Reduction effect of the yield bending moment due to the reduction of prestressing force in the bolts from $0.6f_yA_b$ to zero is presented as follows:

$$\frac{206.62-221.93}{206.62}\times 100=-7.41\%$$

Based on Fig. 8, pre-stressing force has no significant effects on the initial and secondary rotational stiffness values. However, with decreasing in the values of pre-stressing for $0.6f_yA_b$, final and yielding resistant moments are reduced to 7.41%.

5.2 The effects of SMA bolts diameter

Regarding the different diameters of bolts, it should be mentioned that the resistant force of a bolt increases with the increase of its diameter. Extremely increasing of the diameter will result in the non-criticality of the bolts. Therefore, the critical element will control the connection (based on Table 3, the end plate). In this section, the bolts with diameters of 8, 9, 10 and 11mm have been controlled.

According to Fig. 9 and Table 4, the resisting yield moment does not change considering the bolts of over 10mm diameters. Moreover, in the bolts with the diameters more than 10mm, the created rotation is reduced due to the increase of stiffness with the moment remaining constant.

6. Conclusions

The main objective of this research is to analyze the steel connections with extended end plate equipped with 8 dual bolt rows (high strength bolts and shape memory alloy bolts). The analysis is performed using component method presented in EuroCode3. In order to overcome the analytical complexities of nonlinear finite element method while obtaining moment-rotation curve for steel connections and to find the real behavior of moment connections, it is necessary to evaluate the strength, stiffness and ductility of these connections. These necessities are provided by component method. The appropriateness of the results obtained from component method is corroborated through comparing the results with those of finite element method. The results of these two methods differ for 1.4% in the initial rotational stiffness, 9.84% in yield moment and 12.46% in the rotation of yield point. Besides, the effects of the pre-stressing forces applied to the SMA bolts as well as the effects of the bolts diameter are investigated on the moment-rotation curve of connection. If pre-stressing force decreases from $0.6f_yA_b$ to 0, then the resistant yield moment is reduced to 7.41%. If the diameter of SMA bolts augments, the resistant yield moment will increase and become constant after a diameter. Based on the obtained results, it should be mentioned that the studied connection has proper ductility in addition to its strength.

References

Abolmaali, A., Treadway, J., Aswath, P., Lu, F.K. and McCarthy, E. (2006), "Hysteresis behavior of t-stub connections with superelastic shape memory fasteners", *J. Constr. Steel Res.*, **62**(8), 831-838. https://doi.org/10.1016/j.jcsr.2005.11.017.

Aksoylar, N.D., Elnashai, A.S. and Mahmoud, H. (2011), "The design and seismic performance of low-rise long-span frames with semi-rigid connections", *J. Constr. Steel Res.*, **67**(1), 114-126. https://doi.org/10.1016/j.jcsr.2010.07.001.

Arabnejad Khanouki, M.M., Ramli Sulong, N.H. and Shariati, M. (2010), "Investigation of seismic behaviour of composite structures with concrete filled square steel tubular (CFSST) column by push-over and time-history analyses", *Proceedings of the 4th International Conference on Steel & Composite Structures*.

Baei, M. (2014), Seismic Performance of Frames with Extended End-Plate Beam to Column Connection Considering Flexibility of the Connection. M.Sc, University of Tehran.

Bahadori, A.R. and Ghassemieh, M. "Seismic evaluation of I shaped beam-column connection with direct connection", *Proceedings of the 1st Conference on Civil & Architecture Engineering & Urban Sustainable Management*, Gorgan, IRAN, 26 June

Bahadori, A.R. and Ghassemieh, M. (2015), "Seismic evaluation of steel moment frames with end plate moment connection considering connection flexibility by component method", *Proceedings of the 1st International Conference of Steel and Structure*, Tehran, Iran.

Buehler, W.J., Gilfrich, J. and Wiley, R. (1963), "Effect of low-temperature phase changes on the mechanical properties of alloys near composition TiNi", *J. Appl. Phys.*, **34**, 1475-1477. https://doi.org/10.1063/1.1729603.

Christopoulos, C., Filiatrault, A., Uang, C.M. and Folz, B. (2002). "Posttensioned energy dissipating connections for moment-resisting steel frames", *J. Struct. Eng.*, **128**(9), 1111-1120. https://doi.org/10.1061/(ASCE)0733-9445(2002)128:9(1111).

Da Silva, L.S. and Coelho, A.G. (2001), "A ductility model for steel connections", *J. Constr. Steel Res.*, **57**(1), 45-70. https://doi.org/10.1016/S0143-974X(00)00009-2.

Davoodnabi, S.M., Mirhosseini, S.M. and Shariati, M. (2019), "Behavior of steel-concrete composite beam using angle shear connectors at fire condition", *Steel Compos. Struct.*, **30**(2), 141-147. https://doi.org/10.12989/scs.2019.30.2.141.

DesRoches, R., Taftali, B. and Ellingwood, B.R. (2010), "Seismic performance assessment of steel frames with shape memory alloy connections. Part I—analysis and seismic demands", *J. Earthq. Eng.*, **14**, 471-486. https://doi.org/10.1080/13632460903301088.

Ellingwood, B.R., Taftali, B. and DesRoches, R. (2010), "Seismic performance assessment of steel frames with shape memory alloy connections, Part II–Probabilistic seismic demand assessment", *J. Earthq. Eng.*, **14**, 631-645. https://doi.org/10.1080/13632460903247935.

Fanaie, N. and Monfared, M.N. (2016), "Cyclic behavior of extended end-plate connections with shape memory alloy bolts", *Struct. Eng. Mech.*, **60**(3), 507-527. http://dx.doi.org/10.12989/sem.2016.60.3.507.

Fang, C., Yam, M.C., Lam, A.C. and Xie, L. (2014), "Cyclic performance of extended end-plate connections equipped with shape memory alloy bolts", *J. Constr. Steel Res.*, **94**, 122-136. https://doi.org/10.1016/j.jcsr.2013.11.008.

Ghassemieh, M. (1983), Inelastic finite element analysis of stiffened end-plate moment connections.

Ghassemieh, M. and Bahadori, A.R. (2015), "Seismic evaluation of a steel moment frame with cover plate connection considering flexibility by component method", *Proceedings of the 2015 World Congress on Advances in Structural Engineering and Mechanics*, Incheon, Korea.

Gorgun, H. (2013), "Geometrically nonlinear analysis of plane frames composed of flexibly connected members", *Struct. Eng. Mech.*, **45**(3), 277-309. https://doi.org/10.12989/sem.2013.45.3.277.

Hosseinpour, E., Baharom, S., Badaruzzaman, W.H.W., Shariati, M. and Jalali, A. (2018), "Direct shear behavior of concrete filled hollow steel tube shear connector for slim-floor steel beams", *Steel Compos. Struct.*, **26**(4), 485-499. https://doi.org/10.12989/scs.2018.26.4.485.

Hu, J.W., Choi, E. and Leon, R.T. (2011), "Design, analysis and application of innovative composite PR connections between steel beams and CFT columns", *Smart Mater. Struct.*, **20**, 025019.

Jalali, A., Daie, M., Nazhadan, S.V.M., Kazemi-Arbat, P. and Shariati, M. (2012), "Seismic performance of structures with pre-bent strips as a damper", *Int. J. Phys. Sci.*, **7**, 4061-4072. https://doi.org/10.5897/IJPS11.1324.

Khorami, M., Alvansazyazdi, M., Shariati, M., Zandi, Y., Jalali, A. and Tahir, M. (2017), "Seismic performance evaluation of buckling restrained braced frames (BRBF) using incremental nonlinear dynamic analysis method (IDA)", *Earthq. Struct.*, **13**(6), 1-8. http://dx.doi.org/10.12989/eas.2017.13.6.531.

Khorami, M., Khorami, M., Motahar, H., Alvansazyazdi, M., Shariati, M., Jalali, A. and Tahir, M.M. (2017), "Evaluation of the seismic performance of special moment frames using incremental nonlinear dynamic analysis", *Struct. Eng. Mech.*, **63**(2), 259-268. https://doi.org/10.12989/sem.2017.63.2.259.

Khorramian, K., Maleki, S., Shariati, M., Jalali, A. and Tahir, M. (2017), "Numerical analysis of tilted angle shear connectors in steel-concrete composite systems", *Steel Compos. Struct.*, **23**(1), 67-85. https://doi.org/10.12989/scs.2017.23.1.067.

Khorramian, K., Maleki, S., Shariati, M. and Ramli Sulong, N.H.

(2015), "Behavior of tilted angle shear connectors", *PLoS One*, **10**, e0144288. https://doi.org/10.1371/journal.pone.0144288.

Khorramian, K., Maleki, S., Shariati, M. and Ramli Sulong, N.H. (2016), "Behavior of Tilted Angle Shear Connectors (vol 10, e0144288, 2015)", PLOS ONE **11**.

Ma, H., Cho, C. and Wilkinson, T. (2008), "A numerical study on bolted end-plate connection using shape memory alloys", *Mater. Struct*., **41**, 1419-1426. https://doi.org/10.1617/s11527-007-9339-5.

Ma, H., Wilkinson, T. and Cho, C. (2007), "Feasibility study on a self-centering beam-to-column connection by using the superelastic behavior of SMAs", *Smart Mater. Struct*., **16**(5), 1555.

Nasrollahi, S., Maleki, S., Shariati, M., Marto, A. and Khorami, M. (2018), "Investigation of pipe shear connectors using push out test", *Steel Compos. Struct*., **27**(5), 537-543. http://dx.doi.org/10.12989/scs.2018.27.5.537.

Ocel, J., DesRoches, R., Leon, R.T., Hess, W.G., Krumme, R., Hayes, J.R. and Sweeney, S. (2004), "Steel beam-column connections using shape memory alloys", *J. Struct. Eng*., **130**(5), 732-740. https://doi.org/10.1061/(ASCE)0733-9445(2004)130:5(732).

Ölander, A. (1932), "An electrochemical investigation of solid cadmium-gold alloys", *J. Am. Chem. Soc*., **54**, 3819-3833. https://doi.org/10.1021/ja01349a004.

Paknahad, M., Shariati, M., Sedghi, Y., Bazzaz, M. and Khorami, M. (2018), "Shear capacity equation for channel shear connectors in steel-concrete composite beams", *Steel Compos. Struct*., **28(4)**, 483-494. https://doi.org/10.12989/scs.2018.28.4.483.

Penar, B.W. (2005), Recentering beam-column connections using shape memory alloys, Georgia Institute of Technology.

Ricles, J.M., Sause, R., Peng, S. and Lu, L. (2002), "Experimental evaluation of earthquake resistant posttensioned steel connections", *J. Struct. Eng*., **128**(7), 850-859. https://doi.org/10.1061/(ASCE)0733-9445(2002)128:7(850).

Shahabi, S., Ramli Sulong, N.H., Shariati, M., Mohammadhassani, M. and Shah, S. (2016), "Numerical analysis of channel connectors under fire and a comparison of performance with different types of shear connectors subjected to fire", *Steel Compos. Struct*., **20**(3), 651-669. https://10.12989/scs.2016.20.3.651.

Shahabi, S., Ramli Sulong, N.H., Shariati, M. and Shah, S. (2016), "Performance of shear connectors at elevated temperatures-A review", *Steel Compos. Struct*., **20**(1), 185-203. https://doi.org/10.12989/scs.2016.20.1.185.

Shariati, A., Ramli Sulong, N.H., Suhatril, M. and Shariati, M. (2012), "Investigation of channel shear connectors for composite concrete and steel T-beam", *Int. J. Phys. Sci*., **7**, 1828-1831 DOI: 10.5897/IJPS11.1604.

Shariati, A., Ramli Sulong, N.H., Suhatril, M. and Shariati, M. (2012), "Various types of shear connectors in composite structures: A review", *Int. J. Phys. Sci*., **7**(22), 2876-2890. https://doi.org/10.5897/IJPSx11.004.

Shariati, A., Shariati, M., Ramli Sulong, N.H., Suhatril, M., Arabnejad Khanouki, M.M. and Mahoutian, M. (2014), "Experimental assessment of angle shear connectors under monotonic and fully reversed cyclic loading in high strength concrete", *Constr. Build. Mater*., **52**, 276-283. http://dx.doi.org/10.1016/j.conbuildmat.2013.11.036.

Shariati, M. (2013), Behaviour of C-shaped Shear Connectors in Stell Concrete Composite Beams, Jabatan Kejuruteraan Awam, Fakulti Kejuruteraan, Universiti Malaya.

Shariati, M., Ramli Sulong, N.H. and Arabnejad Khanouki, M.M. (2010), "Experimental and analytical study on channel shear connectors in light weight aggregate concrete", *Proceedings of the 4th International Conference on Steel & Composite Structures*, 21 - 23 July, 2010, Sydney, Australia, Research Publishing Services.

Shariati, M., Ramli Sulong, N.H. and Arabnejad Khanouki, M.M. (2012), "Experimental assessment of channel shear connectors under monotonic and fully reversed cyclic loading in high strength concrete", *Mater. Design*, **34**, 325-331 DOI: 10.1016/j.matdes.2011.08.008.

Shariati, M., Ramli Sulong, N.H., Arabnejad Khanouki, M.M. and Mahoutian, M. (2011), "Shear resistance of channel shear connectors in plain, reinforced and lightweight concrete", *Scientific Research and Essays*, **6**, 977-983.

Shariati, M., Ramli Sulong, N.H., Arabnejad Khanouki, M.M. and Shariati, A. (2011), "Experimental and numerical investigations of channel shear connectors in high strength concrete", *Proceedings of the 2011 world congress on advances in structural engineering and mechanics (ASEM'11+)*.

Shariati, M., Ramli Sulong, N.H., Shariati, A. and Arabnejad Khanouki, M.M. (2015), "Behavior of V-shaped angle shear connectors: experimental and parametric study", *Mater. Struct*., **49**, 3909-3926. DOI: 10.1617/s11527-015-0762-8.

Shariati, M., Ramli Sulong, N.H., Shariati, A. and Kueh, A.B.H. (2016), "Comparative performance of channel and angle shear connectors in high strength concrete composites: An experimental study", *Constr. Build. Mater*., **120**, 382-392. https://doi.org/10.1016/j.conbuildmat.2016.05.102.

Shariati, M., Ramli Sulong, N.H., Sinaei, H., Khanouki, A., Mehdi, M. and Shafigh, P. (2011), Behavior of channel shear connectors in normal and light weight aggregate concrete (experimental and analytical study). Advanced Materials Research, Trans Tech Publ.

Shariati, M., Ramli Sulong, N.H., Suhatril, M., Shariati, A., Arabnejad Khanouki, M.M. and Sinaei, H. (2012), "Behaviour of C-shaped angle shear connectors under monotonic and fully reversed cyclic loading: An experimental study", *Mater. Design*, **41**, 67-73. https://doi.org/10.1016/j.matdes.2012.04.039.

Shariati, M., Ramli Sulong, N.H., Suhatril, M., Shariati, A., Arabnejad Khanouki, M.M. and Sinaei, H. (2012), "Fatigue energy dissipation and failure analysis of channel shear connector embedded in the lightweight aggregate concrete in composite bridge girders", *Proceedings of the 5th International Conference on Engineering Failure Analysis*, 1-4 July 2012, Hilton Hotel, The Hague, The Netherlands.

Shariati, M., Ramli Sulong, N.H., Suhatril, M., Shariati, A., Arabnejad Khanouki, M.M. and Sinaei, H. (2013), "Comparison of behaviour between channel and angle shear connectors under monotonic and fully reversed cyclic loading", *Constr. Build. Mater*., **38**, 582-593. https://doi.org/10.1016/j.conbuildmat.2012.07.050.

Shariati, M., Shariati, A., Ramli Sulong, N.H., Suhatril, M. and Arabnejad Khanouki, M.M. (2014), "Fatigue energy dissipation and failure analysis of angle shear connectors embedded in high strength concrete.", *Eng. Fail. Anal*., **41**, 124-134: https://doi.org/10.1016/j.engfailanal.2014.02.017.

Shariati, M., Tahmasbi, F., Mehrabi, P., Bahadori, A. and toghroli, A. (2020), "Monotonic behavior of C and L shaped angle shear connectors within steel-concrete composite beams: an experimental investigation", *Steel Compos. Struct*., **35**(2), 237-247. http://dx.doi.org/10.12989/scs.2020.35.2.237.

Shariati, M., Toghroli, A., Jalali, A. and Ibrahim, Z. (2017), "Assessment of stiffened angle shear connector under monotonic and fully reversed cyclic loading", *Proceedings of the 5th International Conference on Advances in Civil, Structural and Mechanical Engineering-CSM 2017*.

Standard, B. (2006), "Eurocode 3—Design of steel structures—", BS EN 1993-1 **1**, 2005.

Sumner, E.A. and Murray, T.M. (2002), "Behavior of extended end-plate moment connections subject to cyclic loading", *J.*

Struct. Eng., **128**, 501-508.

Tahmasbi, F., Maleki, S., Shariati, M., Ramli Sulong, N.H. and Tahir, M.M. (2016), "Shear Capacity of C-Shaped and L-Shaped Angle Shear Connectors", PLoS One **11**, e0156989. https://doi.org/10.1371/journal.pone.0156989.

Venture, S.J. (1997), SAC. Protocol for Fabrication, Inspection, Testing and Documentation of Beam-Column Connection Test and Other Experimental Specimens. SAC Rep, SAC/BD-97/02, Sacramento, California.

Vernon, L. and Vernon, H. (1941), "Process of manufacturing articles of thermoplastic synthetic resins", US Patent **2234993**.

Wang, S. and Chen, Y. (2009), "Initial stiffness and moment resistance of reinforced joint with end-plate connection", Frontiers of Architecture and Civil Engineering in China, **3**, 345.

Wei, X., Shariati, M., Zandi, Y., Pei, S., Jin, Z., Gharachurlu, S., Abdullahi, M.M., Tahir, M.M. and Khorami, M. (2018), "Distribution of shear force in perforated shear connectors", *Steel Compos. Struct.*, **27**(3), 389-399. http://dx.doi.org/10.12989/scs.2018.27.3.389.

CC

Appendix A The symbols used in this study

A	**Cross section area**
A_s	Tensile stress area of the bolts
A_{vc}	Shear area of the column
$b_{eff,c,wc}$	Effective width of the column web in compression zone
$b_{eff,t,wb}$	Effective width of the beam web in tension zone
$b_{eff,t,wc}$	Effective width of the column web in tension zone
D	Nominal diameter of the bolts
d_c	Clear depth of the column web
d_{M16}	Nominal diameter of a M16 bolt
E	Young's modulus of members
F_y	The force that corresponds to yield
f_{ub}	Ultimate tensile strength of the bolts
f_y	Yield stress
$f_{y,wb}$	Yield stress of a web beam
$f_{y,wc}$	Yield stress of a web column
$F_{T,1,Rd}$	Design tension resistance of a T-stub flange for mode 1
$F_{T,2,Rd}$	Design tension resistance of a T-stub flange for mode 2
k_1 to k_{10}	Stiffness coefficients for basic joint components according to Part 1.8, EuroCode3
K_e	Elastic stiffness of the component, obtained from ki×E, according to Part 1.8, EuroCode3
K_{pl}	Post limit stiffness of the component
L_b	Bolt elongation length
l_{eff}	The smallest effective lengths (individually or as part of a bolt group)
$l_{eff,nc}$	Non-circular pattern effective length
$l_{eff,cp}$	Circular pattern effective length
$l_{eff,1}$	First mode effective length
$l_{eff,2}$	Second mode effective length
$M_{c,Rd}$	Moment resistance of the beam cross-section
$M_{pl,1,Rd}$	Design moment resistance of a T-stub flange for mode 1
$M_{pl,2,Rd}$	Design moment resistance of a T-stub flange for mode 2
m	Distance between the bolt center line and the face of the weld connecting the beam web to the end plate
n_b	Number of bolt rows
t_{fc}	Thickness of column flange
t_p	End plate thickness
t_{wb}	Thickness of web beam
t_{wc}	Thickness of web column
z	Lever arm according to Part 1.8, EuroCode3
β	Transformation parameter according to Part 1.8, EuroCode3
γ_{M0}	Partial safety factor for resistance of class 1, 2 or 3 cross-section
γ_{M1}	Partial safety factor for resistance of member to buckling or resistance of class 4 cross-section
γ_{Mb}	Partial safety factor for resistance of bolted connections
ω	Reduction factor to allow for the possible effects of shear in the column web panel
Δ_f	Deformation that corresponds to failure
Δ_y	Deformation that corresponds to yield
$V_{wp,Rd}$	Design plastic shear design

$F_{t,wb,Rd}$	Design tension resistance of the beam web
$F_{t,Rd}$	Design tension resistance of a bolt according to Table 3.4 of Part 1.8, EuroCode3
$F_{c,wc,Rd}$	Design resistance of an unstiffened column web subjected to transverse compression
$F_{t,wb,Rd}$	Design resistance of an unstiffened column web subjected to transverse tension